

Investigating the negative tension stiffening effect of reinforced concrete

Carlos Zanuy[†]

Department of Continuum Mechanics and Structures, E.T.S. Ingenieros de Caminos, Canales y Puertos, Universidad Politécnica de Madrid, Av. Profesor Aranguren s/n, 28040 Madrid, Spain

(Received November 13, 2008, Accepted November 11, 2009)

Abstract. The behaviour of a reinforced concrete tension member is governed by the contribution of concrete between cracks, tension stiffening effect. Under highly repeated loading, this contribution is progressively reduced and the member response approximates that given by the fully cracked member. When focusing on the unloaded state, experiments show deformations larger than those of the naked reinforcement. This has been referred to as negative tension stiffening and is due to the fact that concrete carries compressive stresses along the crack spacing, even though the tie is subjected to an external tensile force. In this paper a cycle-dependent approach is presented to reproduce the behaviour of the axially loaded tension member, paying attention to the negative tension stiffening contribution. The interaction of cyclic bond degradation and time-dependent effects of concrete is investigated. Finally, some practical diagrams are given to account for the negative tension stiffening effect in reinforced concrete elements.

Keywords: cracking; bond mechanics; reinforced concrete; tension stiffening; repeated loads.

1. Introduction

Cracking is the main characteristic of concrete structures and is due to the small tensile strength of concrete with respect to the compressive one. Cracking affects the design of reinforced concrete since it determines the quantity of reinforcement required to carry the applied loads in ultimate limit state and to control crack widths and deflections in serviceability limit state. Concrete still carries tensile stresses between cracks in service conditions, the tension stiffening effect. Such a contribution plays a significant role, especially in lightly reinforced concrete members, as recently confirmed by (Gilbert 2007).

The behaviour of a tension member is actually governed by the bond-slip mechanism at the steel-concrete interface. As the relative slip between both materials increases, bond stresses develop and longitudinal stresses are transferred from the reinforcement to the effective concrete area. Such transferred stresses are the tension stiffening contribution.

Under monotonic loads, it is well known that a reinforced concrete tie subjected to pure tension behaves somewhere between the load-deformation curves that correspond to the uncracked and fully

[†] Assistant Professor, Ph.D., Research Associate, E-mail: czs@caminos.upm.es

cracked states (so-called states I and II, respectively). The codes of practice (CEB - FIP 1991, CEN 2004) are usually based on empirical interpolations between both states without an explicit consideration of the bond mechanism. As well, advanced theoretical approaches to model concrete structures often include tension stiffening in an indirect way. Such models fall into two main categories: on the one hand, approaches within the European tradition (Ghali and Favre 1994, König and Fehling 1988) use a stress-strain curve for the reinforcement stiffer than the bare steel; on the other hand, smeared models within the American tradition (Vecchio 2000, Vecchio and Collins 1986) assign a larger softening capacity to the average concrete response in tension. Only a few researchers (Kaklauskas and Ghaboussi 2001) have included the influence of further parameters in the formulation of the average concrete stress-strain law, like the amount of reinforcement.

Other detailed models to study the tension stiffening effect do consider the bond-slip behaviour, including general bond models (Balazs 1993) or simplified approaches as the rigid-plastic bond-slip behaviour (Marti P. 1998).

Although the aforementioned models are focused on different details, they all describe well accepted conclusions on the static behaviour. Much smaller has been the research on the response of the reinforced concrete tie under repeated and sustained loads. Besides the long term behaviour of concrete itself, the experimental evidence (Rehm and Eligehausen 1979) shows that bond between concrete and steel deteriorates under repeated loads, leading to increasing crack widths and deformations. Moreover, it has been reported that values under minimum load may become larger than those that correspond to the state II (bare steel) (Günther and Mehlhorn 1990). This result has been called the negative tension stiffening effect and only a few authors have dealt with it (Gómez Navarro and Lebet 2001, Muttoni and Fernández Ruiz 2007). A deeper understanding is required to account for the realistic cyclic bond-slip behaviour and overcome the difficulties presented by the employ of monotonic-based approaches.

Many reinforced concrete elements are subjected to repetitive loading (due to traffic, waves or wind) and their permanent state is represented by the minimum load. The serviceability verification according to current codes of practice may underestimate crack widths and deformations.

In this paper a new cycle-dependent model is presented to solve the reinforced concrete tie under repeated tensile stresses, including the interaction with time-dependent shrinkage. Simplified expressions are also derived to include the negative tension stiffening contribution for practical purposes.

2. Bond mechanics and the reinforced concrete tie

2.1 Monotonic behaviour

In this clause the influence of the bond-slip mechanism on the response of the reinforced concrete tie is analysed. Only a single cycle will be now considered. Fig. 1 shows the behaviour of the tie in terms of the F - ε_m and F - w diagrams. The monotonic behaviour may be subdivided into the next well known stages: uncracked state until f_{ct} is reached at one section; crack formation stage, where the crack pattern develops until the cracks locate at a roughly constant distance s_r to each other; stabilised cracking, where cracks increase their width and the average response approximates the state II as tension stiffening decreases; and plastic stage since the reinforcement yields. The attention will be paid to the stabilised cracking stage due to the fact that this stage is dominant in

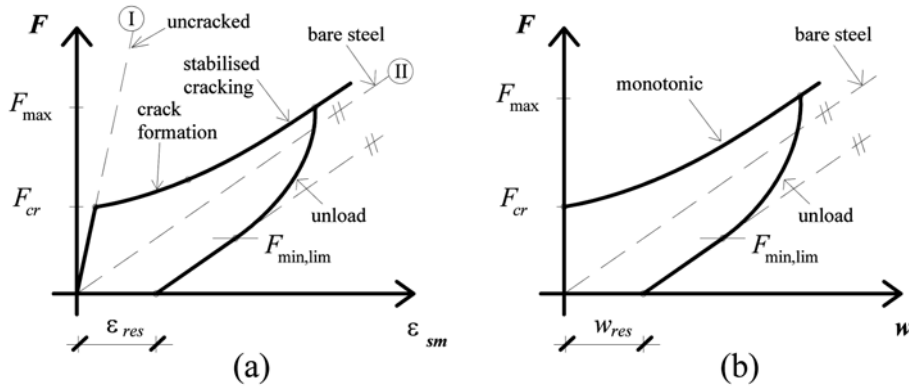


Fig. 1 Behaviour of a reinforced concrete tie. (a) Force-average steel strain, (b) Force-crack width

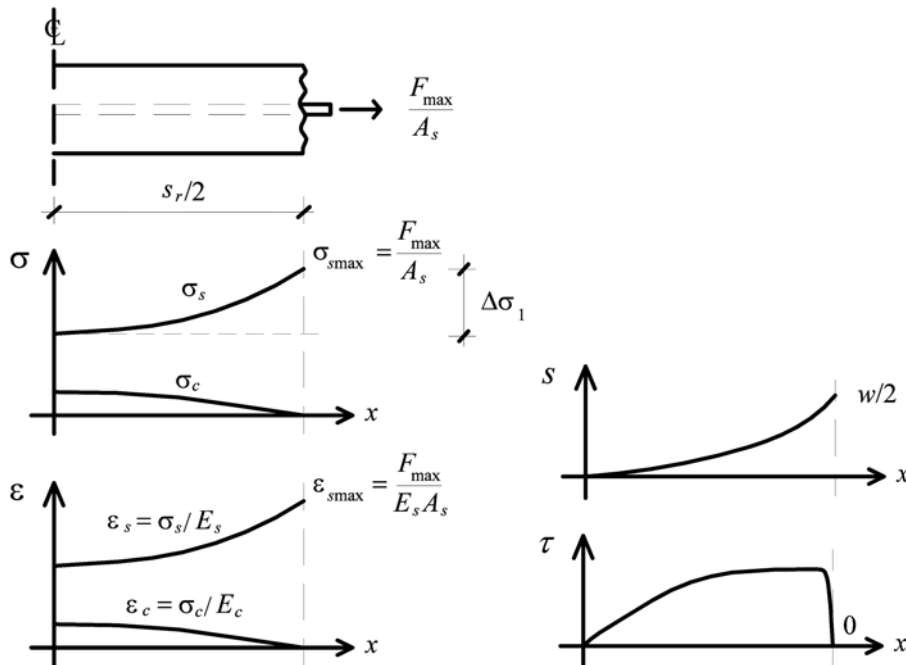


Fig. 2 Distribution of stresses, strains and slips between two adjacent cracks at the stabilised cracking stage

members under service loads.

Under monotonic loading, the tension stiffening contribution reduces the average strain and the crack width with respect to that given by the state II (Fig. 1). This is due to the stresses transferred from the reinforcement to the concrete by bond stresses between two adjacent cracks. The longitudinal distribution of the variables involved in the problem is typically represented in Fig. 2. Due to symmetry, only one half of the crack spacing is represented (note that $\varepsilon_s \neq \varepsilon_c$ along $s_r/2$ and relative slip exists everywhere at this stabilised cracking stage).

The equations governing the response may be written by considering the equilibrium of an arbitrarily chosen differential portion (Balazs 1993, Chan *et al.* 1992, FIB 2000) (Fig. 3(a))

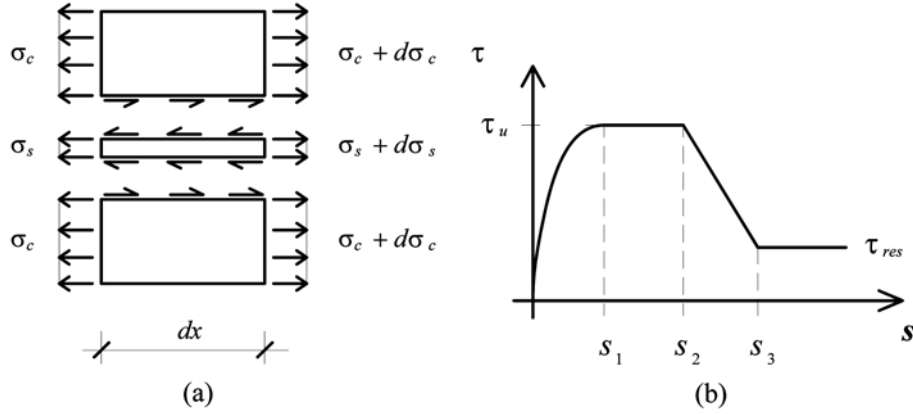


Fig. 3 (a) Stresses at a differential portion of the tie, (b) Bond-slip law according to MC90 (CEB - FIP 1991)

$$\frac{d\sigma_s}{dx} = \tau \frac{U_s}{A_s}; \quad \frac{d\sigma_c}{dx} = -\tau \frac{U_s}{A_c} \quad (1)$$

If linear elastic behaviour of materials between cracks and that concrete cannot carry tensile stresses at the crack (which is realistic under repeated loading owing to the rather fast loss of the softening capacity (Cornelissen and Reinhardt 1984) is assumed, the differential equation and the boundary conditions of the problem may be derived from the strain compatibility equation ($ds/dx = \varepsilon_s - \varepsilon_c \rightarrow d^2s/dx^2 = d\varepsilon_s/dx - d\varepsilon_c/dx$)

$$\frac{d^2s}{dx^2} - \frac{4(1+n\rho)}{E_s\Phi} \tau = 0 \quad (2)$$

$$s(x=0) = 0; \quad \sigma_s(x=s_r/2) = \sigma_{smax}; \quad \sigma_c(x=s_r/2) = 0 \quad (3)$$

where $n = E_s/E_c$ and $\rho = A_s/A_c$. The crack width is twice the slip at the crack. The bond-slip behaviour follows the law plotted in Fig. 3(b) (CEB - FIP 1991), where the first branch is given by

$$\tau = \tau_u \left(\frac{s}{s_1} \right)^\alpha \quad (4)$$

where τ_u is the bond strength, s_1 is the relative slip at the peak bond stress and $\alpha = 0.4$. Particular values for these parameters may be found in the technical literature (CEB - FIP 1991, Kreller 1990). Introducing Eq. (4) into Eq. (2) yields to the following differential equation

$$\frac{d^2s}{dx^2} - \frac{4(1+n\rho)\tau_u s^\alpha}{E_s\Phi s_1^\alpha} = 0 \quad (5)$$

Unfortunately an explicit solution of Eq. (5) cannot be derived (refer to Appendix I). Some authors have obtained analytical expressions by introducing some simplifications, such as the tension chord model (Marti *et al.* 1998b) based on a rigid-plastic bond-slip law, or the employ of a piecewise linear approximation of the bond-slip law (Yankelevsky *et al.* 2008).

In this paper a numerical solution of the general problem is used, as schematised in Fig. 4. The algorithm is based on that suggested by (Tassios and Yannopoulos 1981). The half of the crack

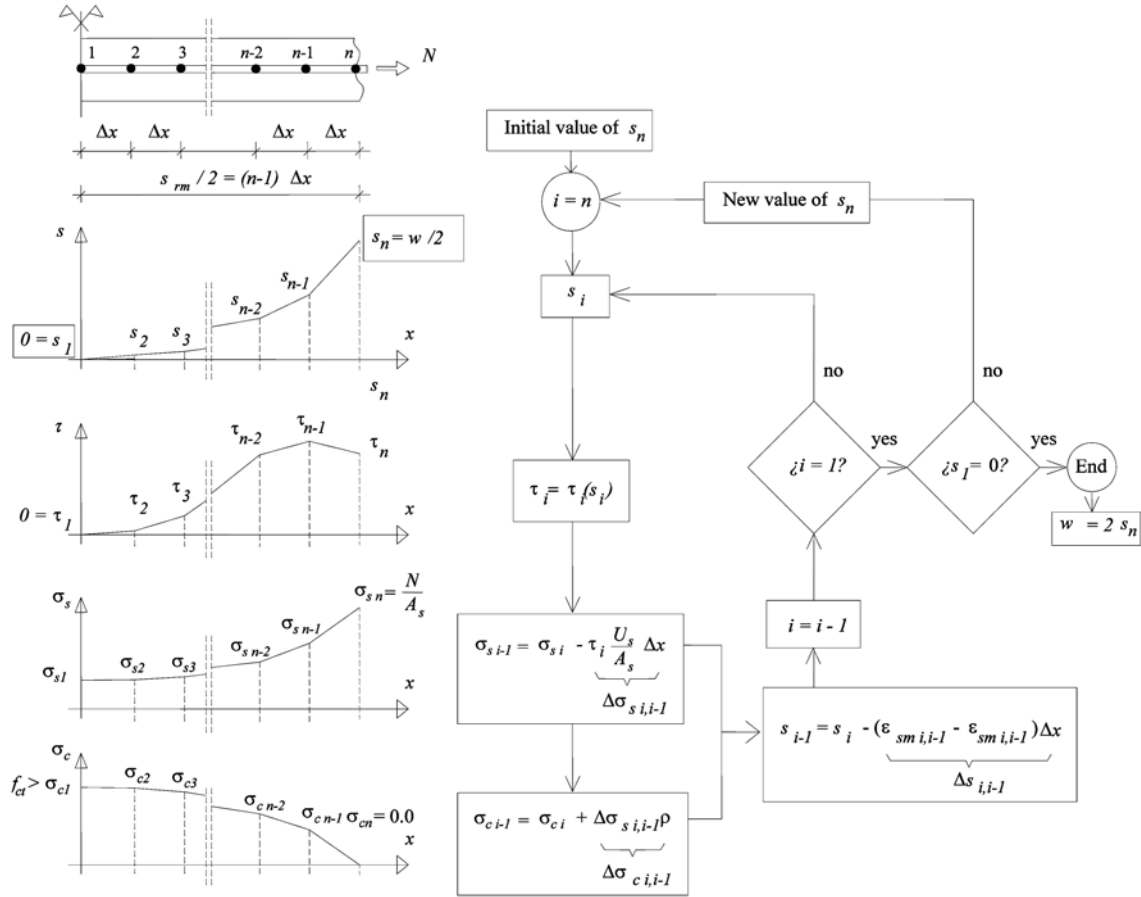


Fig. 4 Flow chart of the numerical algorithm to solve the reinforced concrete tie

spacing is divided into n nodes and $n - 1$ parts of constant length Δx . A trial value of the slip at the crack (i.e., of the crack width, since $w = 2s_n$) is introduced, and the values of stresses, strains and slip are computed following the flow chart of Fig. 4 until the slip at the section halfway between cracks is estimated ($i = 1$). If such a value is zero (or less than an accepted tolerance) the solution has been found. Otherwise a new trial value for s_n is introduced. The iterations can be done employing the regula-falsi algorithm, which is easily programmed and provides excellent robustness and very small consuming times.

2.2 Negative tension stiffening

The unloading stage of Fig. 1 is now considered. It is observed that the average strain and the crack width become larger than those obtained in an unbonded tie (state II, bare steel), which has been referred to as the negative tension stiffening effect. The distribution of stresses under minimum load is represented in Fig. 5(a) (values under maximum load are also plotted by discontinuous lines). Two situations may be obtained, depending whether the minimum force is larger or smaller than the so-called limit minimum stress, $\sigma_{\min, \lim}$.

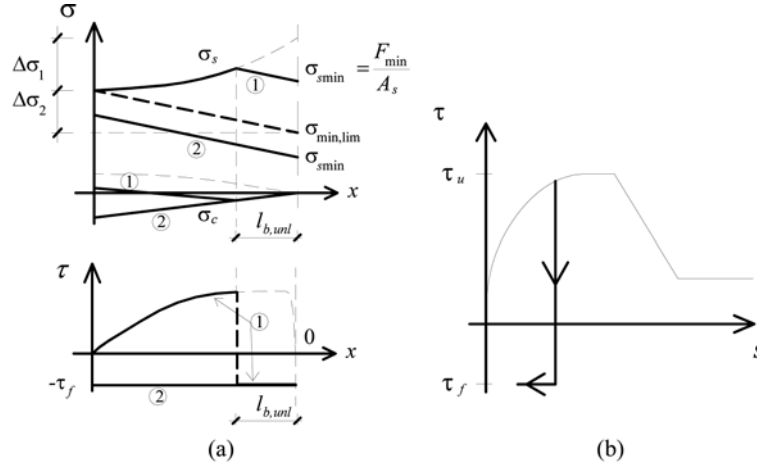


Fig. 5 (a) Distribution of stresses under minimum load, (b) Unloading bond-slip law

The behaviour is governed by the unloading branch of the bond-slip law, which may be considered linear down to the negative frictional strength ($\tau_f = 0.15-0.25\tau_u$, according to (Morita and Kaku 1973, Plaines *et al.* 1982)). In this paper a vertical unloading line is considered (Fig. 5b), as suggested by (Pochanart and Harmon 1989). The numerical solution of the problem in the unloading stage may be found by the employ of the algorithm of Fig. 4 just by introducing the unloading bond-slip behaviour.

If the minimum load is larger than the limit minimum stress (case 1 of Fig. 5(a)), the unloaded transfer length is smaller than half of the crack spacing ($l_{b,unl} < s_r/2$). When the minimum load is smaller than the limit minimum stress (case 2 of Fig. 5(b)), the unloaded transfer length is equal to the half of the crack spacing ($l_{b,unl} = s_r/2$) and the bond stress is constant along $s_r/2$ ($\tau = -\tau_f$). It must be noted that in this situation concrete carries compressive stresses, even though the tie is subjected to a tensile axial force F_{min} .

Since the bond stress is constant in the second case, the distribution of concrete and steel stresses follows straight lines (Fig. 6). An explicit solution of this second case may be therefore derived. Let ΔF_b be the axial force transferred from the steel to the concrete by the negative bond stress along $s_r/2$

$$\Delta F_b = \tau_f U_s \frac{s_r}{2} \quad (6)$$

At the section halfway between cracks, the steel and concrete stress increments with respect to the cracked section are, respectively (Fig. 6)

$$\Delta\sigma_2 = \frac{1}{2}s_r \tau_f \frac{U_s}{A_s} = \frac{2s_r \tau_f}{\Phi} \quad (7)$$

$$\Delta\sigma_c = \frac{1}{2}s_r \tau_f \frac{U_s}{A_c} = \Delta\sigma_2 \rho \quad (8)$$

Hence

$$\Delta \varepsilon_s = \frac{2s_r \tau_f}{E_s \Phi}; \quad \Delta \varepsilon_c = \frac{2s_r \tau_f \rho}{E_c \Phi} \quad (9)$$

And the average strains of the steel and the concrete become

$$\varepsilon_{sm} = \frac{\sigma_{s \min}}{E_s} + \frac{1}{2} \Delta \varepsilon_s = \frac{\sigma_{s \min}}{E_s} + \frac{s_r \tau_f}{E_s \Phi} \quad (10)$$

$$\varepsilon_{cm} = \frac{1}{2} \Delta \varepsilon_c = \frac{s_r \tau_f \rho}{E_c \Phi} \quad (11)$$

The second term of Eq. (10) provides the strain increase with respect to the strain of the naked reinforcement, i.e. the negative tension stiffening contribution. Besides, the smallest steel stress along the tie locates at the crack. The shape of Eq. (10) shows that, when the minimum load is smaller than the limit minimum force, the F - ε_{sm} diagram is a straight line parallel to that corresponding to the state II (Fig. 1(a)). Moreover, the residual average strain is

$$\varepsilon_{res} = \frac{s_r \tau_f}{E_s \Phi} \quad (12)$$

From Fig. 6 and Eqs. (10)-(11), the minimum crack width may be also estimated

$$w_{\min} = 2 \int_0^{s_r/2} (\varepsilon_s - \varepsilon_c) dx = 2(\varepsilon_{sm} - \varepsilon_{cm}) \frac{s_r}{2} = \left(\frac{\sigma_{s \min}}{E_s} + \frac{s_r \tau_f}{E_s \Phi} + \frac{s_r \tau_f \rho}{E_s \Phi} \right) s_r \quad (13)$$

Hence,

$$w_{\min} = \frac{\sigma_{s \min} s_r}{E_s} + \frac{\tau_f s_r^2}{E_s \Phi} (1 + n\rho) \quad (14)$$

The increase of the crack width due to the negative tension stiffening is given by the second term of Eq. (14). It is again obtained that the F - w curve follows a straight line parallel to that represented by the bare steel if $F_{\min} < F_{\min, \lim}$ (Fig. 1(b)). The residual crack width yield

$$w_{res} = \frac{\tau_f s_r^2}{E_s \Phi} (1 + n\rho) \quad (15)$$

The practical implications of these equations are studied in section 5.

The limit minimum stress may be defined as

$$\sigma_{\min, \lim} = \sigma_{s \min} - (\Delta \sigma_1 + \Delta \sigma_2) \quad (16)$$

where $\Delta \sigma_1$ is the maximum stress transferred from the reinforcement to the concrete under maximum load (refer to Fig. 2 or Fig. 5(a)) and $\Delta \sigma_2$ is given by Eq. (7) (see Fig. 5(a) or Fig. 6). The value of $\Delta \sigma_1$ cannot be obtained by a closed expression and is here estimated by using the numerical algorithm referred to in section 2.1. The influence of some parameters on $\sigma_{\min, \lim}$ is investigated in Fig. 7. Good bond properties are assumed in this example. The crack spacing is introduced as dependent on the geometry ($s_r = \Phi / (3.6\rho)$) according to Model Code (CEB - FIP 1991). The smaller the steel reinforcement ratio, the lower the minimum limit stress; and the smaller the diameter, the higher the minimum limit stress.

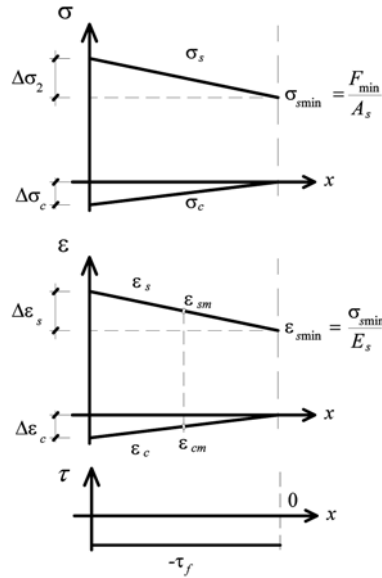


Fig. 6 Distribution of stresses and strains under minimum load when $l_{b,lim} = s_r/2$

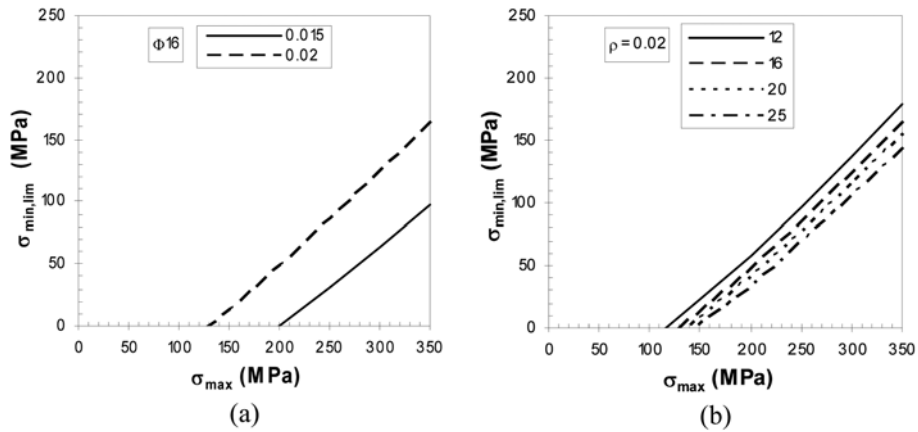


Fig. 7 Analysis of $\sigma_{min,lim}$ ($f_c = 35$ MPa, $\tau_u = 2f_c^{0.5}$, $\tau_f = 0.15 \tau_u$, $s_1 = 0.6$ mm): (a) Influence of ρ , (b) Influence of Φ

3. Tie model under highly repeated loading

The increase of crack widths and deformations of a reinforced concrete tie under repeated loading is due to the progressive deterioration of the bond properties, which reduces the stress transfer from the steel to the concrete. The typical result of a cyclic pull-out test where the bond stress oscillates between constant limits is plotted in Fig. 8(a), according to (Balazs 1991). The slip grows as the number of cycles increases, with negligible stiffness degradation. Oh and Kim (2007) tested up to pull-out failure specimens that had been previously subjected to constant amplitude cycles. The resulting behaviour is schematised in Fig. 8(b). It can be considered that the response is composed

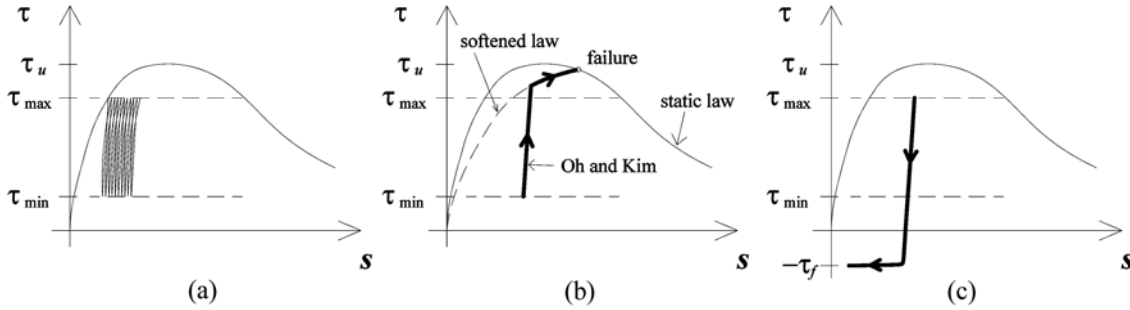


Fig. 8 (a) Bond behaviour under repeated loading, (b) Subsequent reloading, (c) Subsequent unloading

by a straight line with the undamaged stiffness followed by a softened bond-slip law (dashed line in Fig. 8(b)). In addition, the static curve was shown to work as the failure envelope of the cyclic process. If the specimen is unloaded (Fig. 8(c)), the straight line is traced down to the negative frictional strength, following thereafter a horizontal line (Morita and Kaku 1973).

According to the experimental behaviour depicted in Fig. 8, a cyclic bond model is here proposed. The model is composed by a slip evolution law, coupled with softened bond-slip curve and unloading-reloading rule. The slip evolution law provides the slip increase as a function of the number of cycles. The linear trend in double logarithmic scale proposed by (Sippel 1996) is considered

$$s_N = s_0(1 + N)^b \quad (17)$$

$$b = \begin{cases} 0.11; & \tau_{\max}/\tau_u < 0.45 \\ 0.35 \tau_{\max}/\tau_u - 0.05; & \tau_{\max}/\tau_u \geq 0.45 \end{cases} \quad (18)$$

where s_0 is the static slip estimated with Eq. (4), s_N is the total slip after N cycles and b defines the cyclic rate as a function of the maximum bond stress. A similar rule is chosen to define the softened bond-slip law after N cycles. Such a law is defined by updating the characteristic slip s_1 (refer to Fig. 3(b)) as follows

$$s_{1N} = s_1(1 + N)^b \quad (19)$$

Since the static bond-slip law is the failure envelope of the cyclic process, the bond strength reduces when $s_{1N} > s_2$ (Fig. 9).

For the unloading and reloading branches, vertical lines are assumed without cyclic reduction of the stiffness. These branches are limited by the negative frictional strength and the softened bond-slip law, respectively.

A three step numerical procedure is introduced to solve the cyclic problem. The total number of cycles is subdivided into sets of cycles (say ΔN_j each set j). The discretization of the tie given in Fig. 4 is taken into account. The three steps to obtain the influence of one set of cycles j are explained with the help of Fig. 10. For a better understanding, concrete and steel have been drawn separately. To clarify the bond mechanism, a fictitious spring represents the connection at node i .

In the first step the free slip increase of the bond element is allowed as if the concrete and the

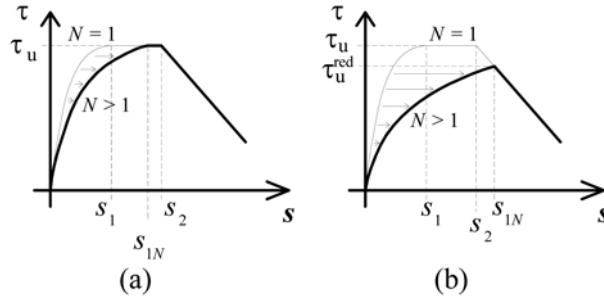


Fig. 9 Cyclic degradation of the bond-slip law

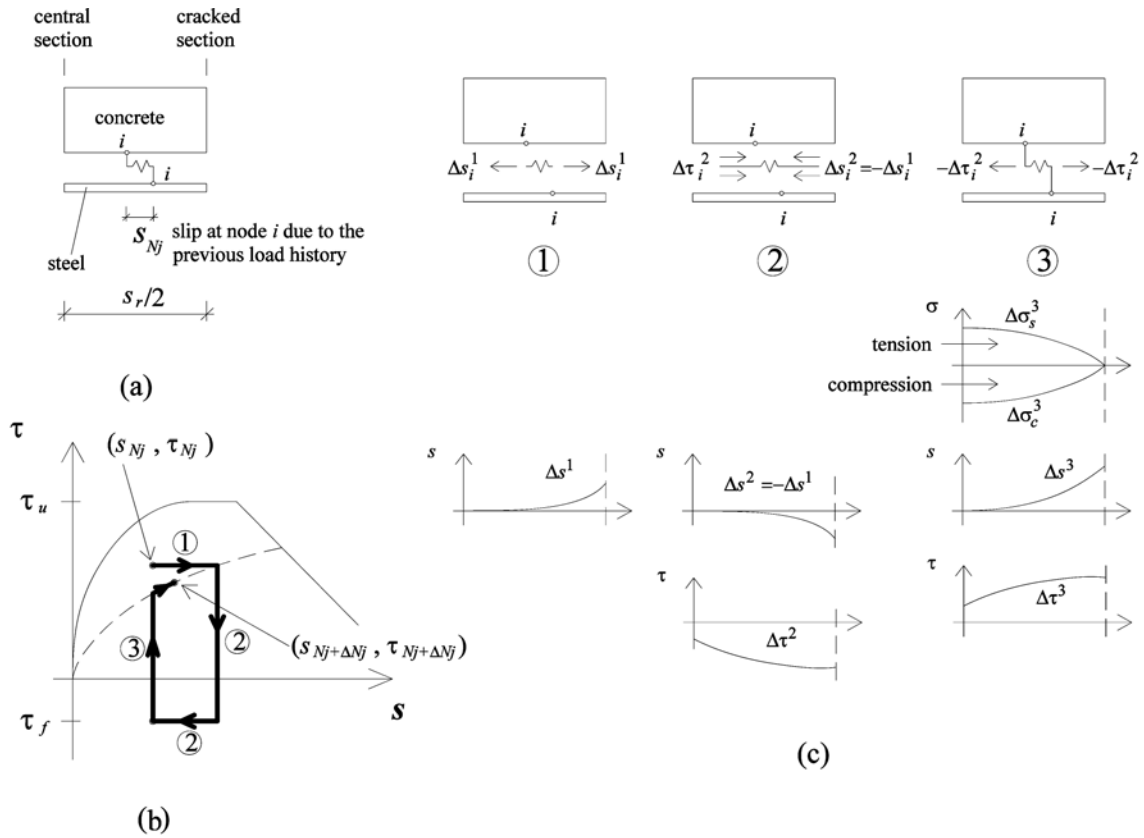
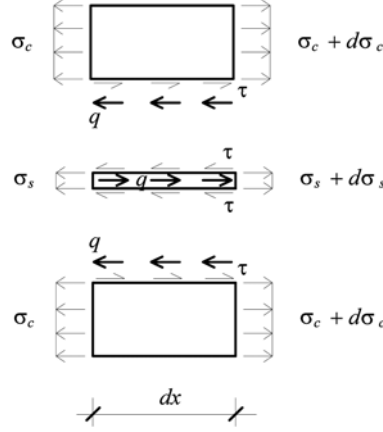


Fig. 10 Three step procedure to solve the tie under repeated loading. (a) Scheme of the concrete-steel-connection, (b) Effect on a single section i , (c) Description of the three steps

steel were not connected, i.e., a free elongation of the fictitious spring takes place and no bond stresses develop. Therefore, concrete and steel do not experiment changes. Of course strain compatibility ($ds/dx = \epsilon_s - \epsilon_c$) is not verified in this step. The free slip increase is estimated from Eq. (17)

$$\Delta s_i^1 = s_{N_j + \Delta N_j} - s_{N_j} \tag{20}$$


 Fig. 11 Differential tie subjected to distributed bond stress q

The free slip increase of the step 1 is fully restrained in the step 2. To do this, restraining bond forces are applied to the fictitious spring elements. Such bond stresses are estimated by employing the assumed unloading behaviour (Fig. 10(b))

$$\Delta \tau_i^2 = -(\tau_{N_j} + \tau_f) \quad (21)$$

$$\Delta s_i^2 = -\Delta s_i^1 \quad (22)$$

The result of steps 1 and 2 is no slip increase (the strain compatibility is recovered), but equilibrium is not verified due to the presence of bond stresses $\Delta \tau_i^2$. Such stresses are applied in reversed directions to the re-connected steel-concrete tie in the third step to restore equilibrium. The third step represents a reinforced concrete tie subjected to imposed bond stress at the level of the steel-concrete interface. The equations that govern such a problem are obtained from equilibrium of a differential portion of the tie (Fig. 11)

$$\frac{d\sigma_s}{dx} = (\tau - q) \frac{U_s}{A_s} \quad (23)$$

$$\frac{d\sigma_c}{dx} = -(\tau - q) \frac{U_s}{A_c} \quad (24)$$

where $q = -\Delta \tau_i^2$ and the reloading bond-slip law is considered as assumed. The algorithm of Fig. 4 solves the problem of the third step just by introducing such particularities.

The addition of the three steps of Fig. 10(c) is the effect of the ΔN_j cycles. As it can be noted (Fig. 10(b)), bond stresses reduce as the relative slip increases. This increase is lower than the free slip of the first step owing to the restriction of the bond mechanism. The result is that lower stresses are transferred from the reinforcement to the concrete and the tension stiffening contribution decreases. The numerical model leads to very fast results when the sets of cycles are chosen such as $N_j = 10^7$. To estimate the values under minimum load, the unloading stage is solved as previously explained, assuming a vertical unloading line followed by a horizontal branch at $\tau = -\tau_f$ (refer to Fig. 5(b)).

The overall behaviour will be explained with the analysis of existing experimental results. The specimen tested by (Blaschke and Mehlhorn 1995) is considered in Fig. 12. It consists of a 20 mm diameter bar embedded into a 1.0 m length prismatic concrete tie (cross section = 0.14 × 0.14 m). It was subjected to 10⁴ load cycles and the oscillation was such as the steel stresses at the crack were $\sigma_{smax} = 285.71$ MPa and $\sigma_{smin} = 57.14$ MPa. The post-treatment of the specimen ensured negligible shrinkage strain during the test.

Three cracks formed (see the first branch of the $\sigma_s - \epsilon_{sm}$ diagram in Fig. 12(a)), being $s_r = 0.23$ m.

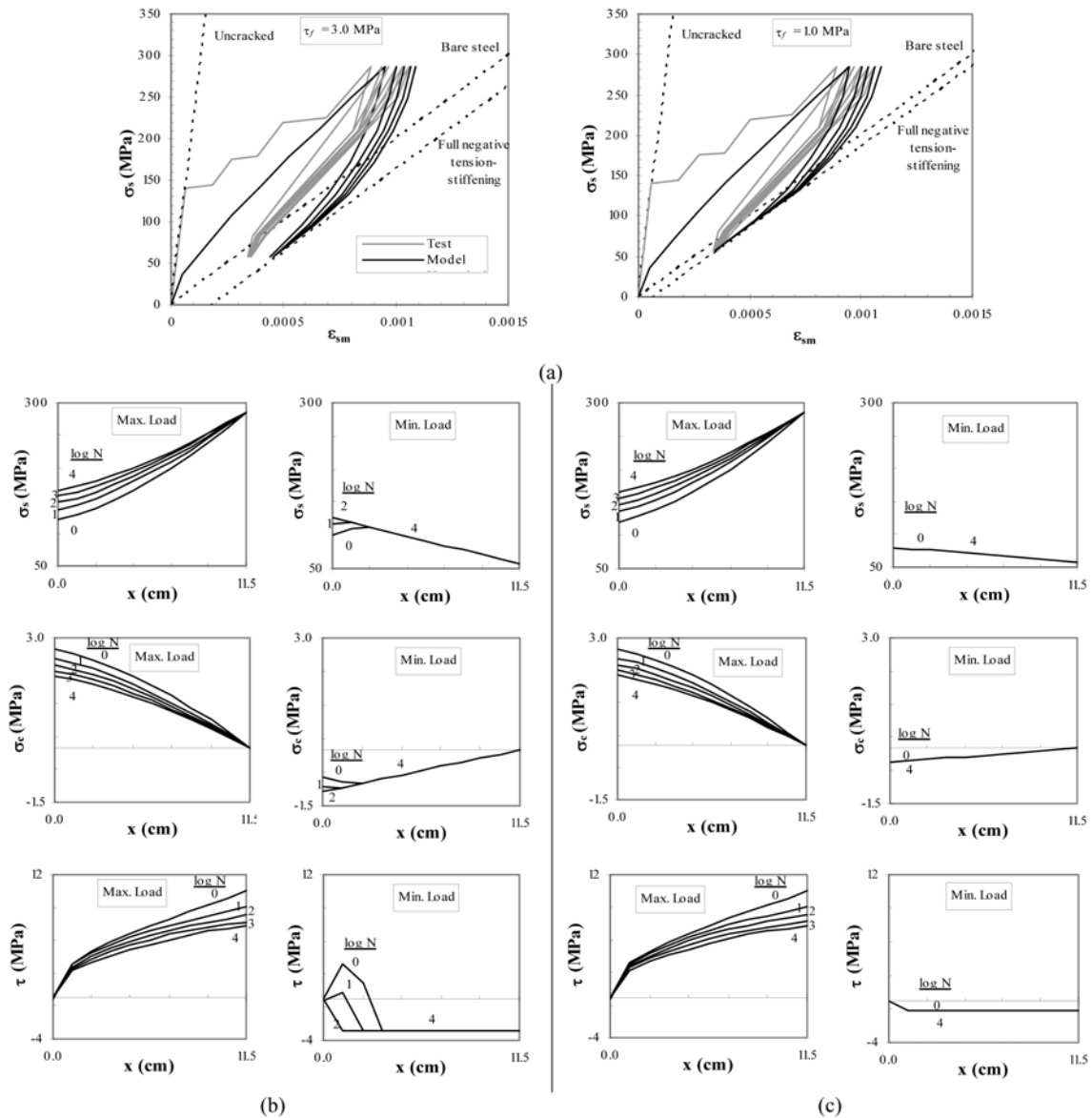


Fig. 12 Interpretation of test results from (Blaschke and Mehlhorn 1995): (a) Cyclic $\sigma_s - \epsilon_{sm}$ diagrams considering $\tau_f = 3.0$ and 1.0 MPa, (b) Model results considering $\tau_f = 3.0$ MPa, (c) Model results considering $\tau_f = 1.0$ MPa

The bond properties were not reported, but good bond behaviour has been adopted to model the test ($\tau_u = 2.5f_c^{0.5}$, $s_1 = 0.25$ mm, $f_c = 35$ MPa). Two values of the negative frictional strength have been considered in order to study its influence ($\tau_f = 3.0$ and 1.0 MPa).

Fig. 12(a) compares the experimental $\sigma_s - \varepsilon_{sm}$ curves with the model results at $N = 1, 10, 100, 1000$ and 10000 . It can be observed that the model does not reproduce the crack formation stage in the first cycle due to the assumption of stabilised cracking since the beginning. The influence of this fact is not relevant under repeated loading. Fig. 12(b) and c represent the evolution of σ_s , σ_c and τ along $s_r/2$ under τ_f maximum and minimum load considering $\tau_f = 3.0$ and 1.0 MPa, respectively.

The experimental results show the progressive degradation of tension stiffening under maximum load, leading to larger values of the average strain. This result is correctly reproduced by the numerical model, and is due to the cyclic reduction of bond stresses and the subsequent increase of steel stresses between cracks.

Under minimum load, the experimental average strain does not experiment an appreciable growth. This indicates that σ_{smin} is very closed to $\sigma_{min,lim}$. When $\tau_f = 1.0$ MPa is adopted in the model, the limit minimum stress is $\sigma_{min,lim} = 97.59$ MPa. Since $\sigma_{smin} < \sigma_{min,lim}$ the full negative tension stiffening capacity is reached in the unloading stage of the first cycle. Due to the fact that no cyclic degradation of τ_f is considered, the model leads to constant values under minimum load during the test (refer to Fig. 12(c)) and the results correspond to those given by Eqs. (10) and (14). Such values agree well with the measured minimum strain.

Interesting findings are obtained when $\tau_f = 3.0$ MPa is considered (Fig. 12(b)). In this case the limit minimum stress is $\sigma_{min,lim} = 51.59$ ($\sigma_{smin} > \sigma_{min,lim}$) and the unloaded transfer length is smaller than $s_r/2$ at the first cycle. The cyclic process decreases the stress transfer, which was called $\Delta\sigma_1$ in Eq. (16). Due to this reduction, the unloaded transfer length increases with number of cycles, which can be also understood as the cyclic growth of $\sigma_{min,lim}$. The situation of $l_{b,unl} = s_r/2$ is reached before $N = 100$ load cycles and the full negative tension stiffening is thereafter developed.

The analysis shows that the progressive bond degradation leads to the situation of $l_{b,unl} = s_r/2$ under cyclic loading, even when $\sigma_{smin} > \sigma_{min,lim}$. Therefore, Eqs. (10) and (14) may be used to represent the long term state of the tension member under minimum load regardless of the stress level. It is worth noting that the employ of a cycle dependent reduction of τ_f would lead to decreasing crack widths and deformations. Further comments on the sensitivity of these formulae are given in section 5.

4. Influence of shrinkage

4.1 Isolated effect of shrinkage

The long term effect of concrete is considered as governed by shrinkage; creep deformations are not accounted for since they have shown to very small owing to the low tensile stresses of concrete between cracks (Beeby and Scott 2006, Fernández Ruiz 2003).

When dealing with the shrinkage influence on a reinforced concrete tie, two situations must be taken into account: before cracking and after cracking. Before cracking the bond-slip mechanism is not involved and perfect bond between concrete and steel may be assumed. In this case the effect of shrinkage is well known and published elsewhere (Ghali and Favre 1994), resulting in additional compressive stresses at the steel, tensile stresses at the concrete (which may cause cracking) and

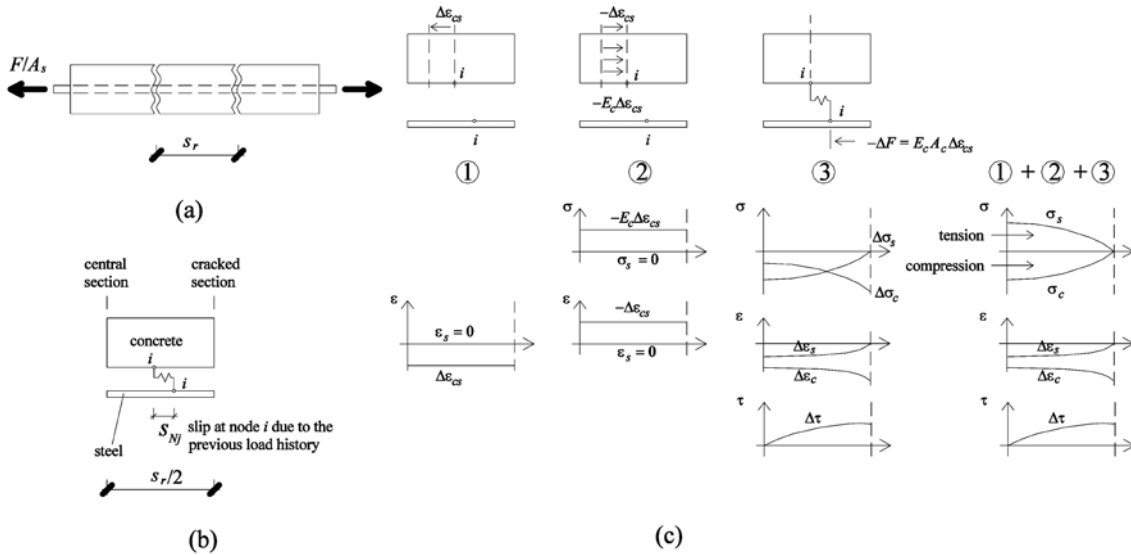


Fig. 13 (a) Cracked reinforced concrete tie, (b) Parts of the tie, (c) Three step procedure to solve the tie under time-dependent shrinkage

overall compressive strains.

The effect of shrinkage after cracking is influenced by the bond-slip mechanism. To study it, it will be assumed that a load is immediately applied to the tie after casting. Shrinkage develops thereafter. It is supposed that stabilised cracking is reached with the first load. A three step model similar to that presented in section 3 is employed. Now the life is subdivided into time intervals Δt_j .

Fig. 13(a) plots the scheme of the reinforced concrete tie with the external load F . The steel stress at the crack remains constant (F/A_s). As previously depicted in Fig. 10(a), the constituents of the tie are represented in Fig. 13(b).

The three steps of the model are drawn in Fig. 13(c). The first step is a free compressive strain increment of the concrete due to the time-dependent shrinkage. This free strain is fully restraint in the second step by applying a restraining force to the concrete ($\Delta F = -E_c A_c \Delta \epsilon_{cs}$). Finally this force is applied in reversed direction to the re-connected steel-concrete tie. In this third step bond stresses develop as the relative slip increases. The slip increase is due to the fact that the compressive steel strain increment is higher than that experimented by the concrete, and therefore $\Delta \epsilon_s - \Delta \epsilon_c > 0$. The result is the progressive increase of the crack width and the formation of self equilibrating stresses: compression at the steel and tension at the concrete. However, it should be noted that the overall result is a shortening of the tie in terms of the average steel strain ϵ_{sm} .

The model results are illustrated by means of a numerical example (Fig. 14). The formulae of the Eurocode EC-2 (CEN 2004) for the shrinkage strain have been taken into account, giving $\epsilon_{cs}(\infty) = -653 \times 10^{-6}$. The evolution of the average strain and the crack width with time is represented in Fig. 14(a) and Fig. 14(b). The distribution of stresses and strains along the half of the crack spacing is plotted in Figs. 14(c)-(f). One aspect that should be kept in mind is the time-dependent development of concrete compressive strains and tensile stresses. The latter could result in the formation of new cracks if f_{ct} were reached. The increase of concrete stresses is due to larger bond stresses, which are accompanied by higher relative slip between concrete and steel: although $\epsilon_c(t) < \epsilon_c(t_0)$, $\epsilon_s(t) - \epsilon_c(t) > \epsilon_s(t_0) - \epsilon_c(t_0)$, which leads to increasing slips (refer to Fig. 14(f)).

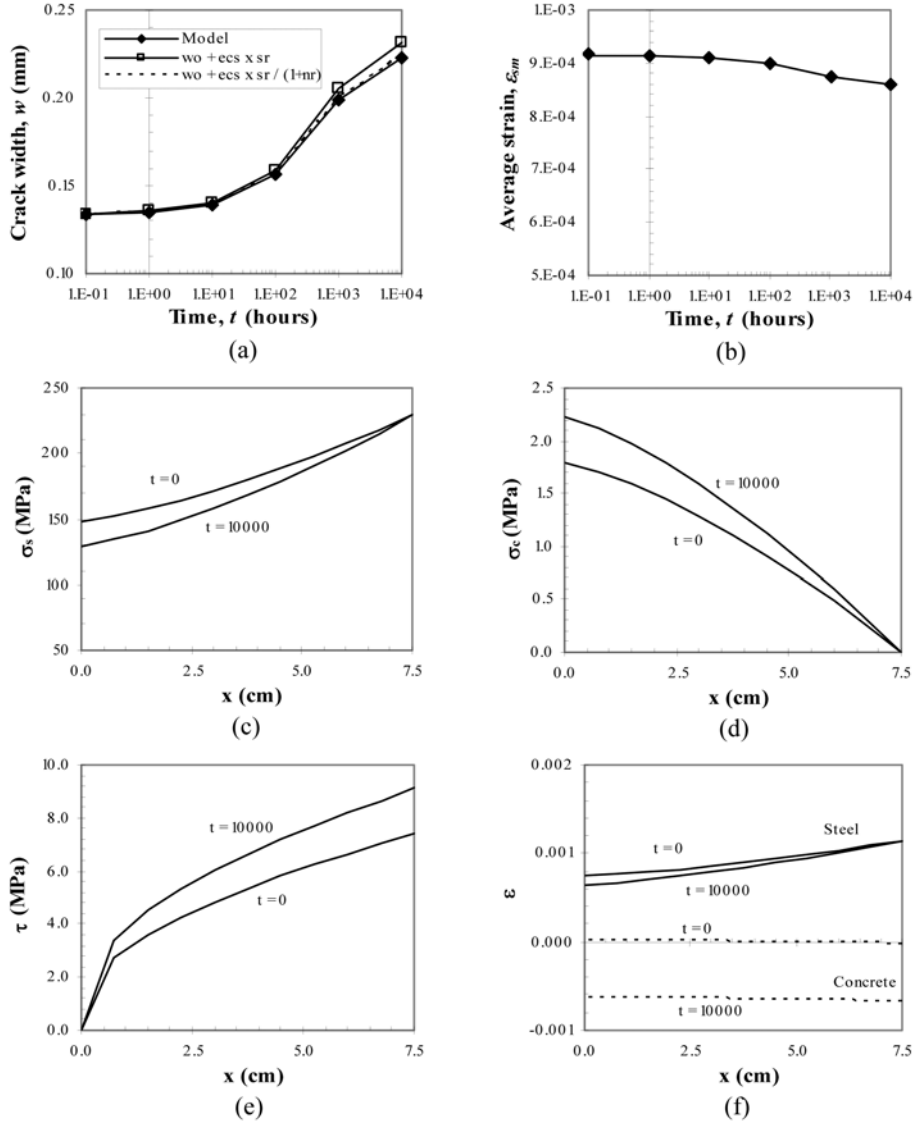


Fig. 14 Effect of shrinkage on a reinforced tie ($\Phi = 20$ mm, $l = 0.12$ m, $s_r = 0.15$ m, $\varepsilon_{cs}(\infty) = -636 \times 10^{-6}$, $F = 72$ kN, $f_c = 120$ MPa, $\tau_u = 2f_c^{0.5}$, $s_1 = 1.0$ mm). (a) Time-dependent crack width, (b) Time-dependent average strain, (c) Distribution of steel stresses, (d) Distribution of concrete stresses, (e) Distribution of bond stresses, (f) Distribution of steel and concrete strains

From Fig. 14(a) it can be concluded that the time-dependent crack width may be estimated by means of the following simplified expression:

$$w(t) = w_0 - \varepsilon_{cs}(t) \frac{s_r}{1 + n\rho} \tag{25}$$

A result that requires further investigation is the encountered reduction of the average strain (Fig. 14(b)). To explain this apparently surprising result, the experiments of a comprehensive study

on long term effects are taken into account (Beeby and Scott 2006). They tested axially reinforced concrete members subjected to pure tension, focusing on the time-dependent response. The specimens were made in pairs: from each pair one specimen was loaded in three stages and the other in a single step. Every loading stage was followed by a period of time in which the load remained constant. The specimens tested in three stages experimented long term strain increase, as generally accepted. The analysis showed that this increase was due to either the formation of new cracks or so-called sudden events. Only a negligible part was due to progressive increase attributed to creep. Sudden events were identified as internal damage leading to abrupt localised strain increases and they could be due to the presence of weak internal zones characterised by small τ_u or f_{ct} . Moreover, the instantaneous strain of the specimens tested in a single step was observed equal to the strain reached in the third step of the three-time loaded specimens. This means that time-dependent strains measured in the periods of smaller load are not expected to occur at the stabilised cracking stage. So the final deformations for the two loading histories were almost the same and the long term fraction was very small and attributed to internal cumulative damage (Beeby and Scott suggested the reduction in tensile strength with time and negligible creep deformation).

Specimens T20R3 (with three loading steps) and T20B3 (with a single step) of (Beeby and Scott 2006) are now considered. Their geometry and maximum load level are those employed in the example of Fig. 14. The experimental long term strain increments were 47×10^{-6} and 75×10^{-6} , respectively. Such values are very small and were assigned to internal damage since new cracks did not appear. The hypothesis of stabilised cracking is assumed in the model of the present paper and the computed effect of shrinkage was evaluated as -54×10^{-6} in Fig. 14(b). This reduction is also very small and can be assumed that the addition of the internal cumulative damage reported by Beeby and Scott would lead to the final strain experimentally measured.

As a conclusion, the time-dependent effect will be considered as the time-dependent crack width of Eq. (25) and negligible change of the average strain. In agreement with (Beeby and Scott 2006), the consideration of long term effects in axially loaded members by factoring the short term strain may be a somewhat questionable procedure (obviously, this conclusion is not valid for members subjected to flexural load).

4.2 Coupled effect of shrinkage and repeated loads

The interaction of time-dependent concrete shrinkage and cycle-dependent degradation of the bond-slip mechanism is accounted for in this clause. For the prediction of the results the simultaneous development of both effects is considered. Each set of cycles ΔN_j is also considered as a time increment $\Delta t_j = \Delta N_j / f$, f being the load frequency. The solution of the problem is quite straightforward just by introducing the shrinkage strain increment of concrete and its corresponding effects (Fig. 13) in the three step model of Fig. 10.

The model capabilities are explored with a numerical example (Fig. 15). The lack of experimental results dealing with the studied subject avoids the comparative verification. The example has been chosen such as the unloaded state verifies $l_{b,unl} = s_r/2$ since the first cycle. Owing to this fact, the stresses remain constant under minimum load during the cyclic process (Fig. 15(c)). However, concrete shrinkage causes the progressive increase of the minimum crack width. The result under maximum load is very similar to that explained in section 3, showing the progressive reduction of tension stiffening (Fig. 15(b)), with an additional crack width growth due to the shrinkage.

The comparison of the model results with simplified expressions (Fig. 15(a)) allows for the

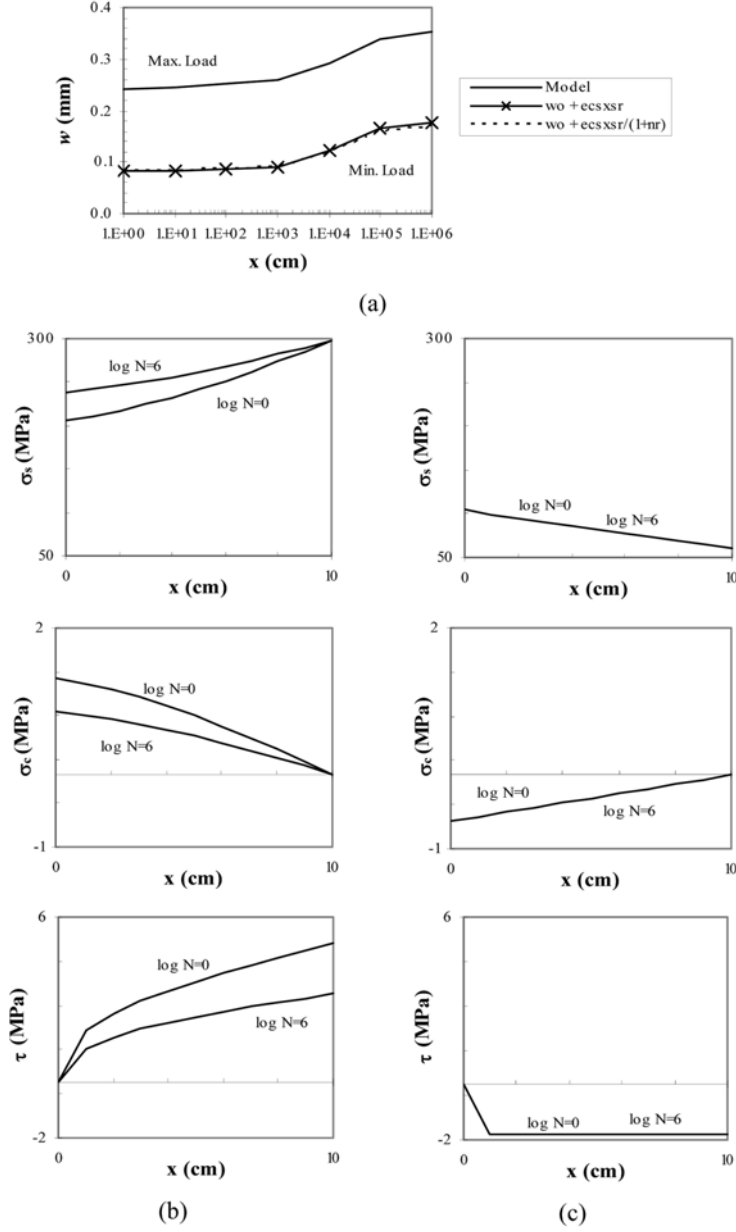


Fig. 15 Interaction of shrinkage and cyclic bond degradation ($\Phi = 20$ mm, $l = 0.12$ m, $s_r = 0.20$ m, $\varepsilon_{cs}(\infty) = -456 \times 10^{-6}$, $F_{\max} = 60$ kN, $F_{\min} = 12$ kN, $f_c = 35$ MPa, $\tau_u = 2f_c^{0.5}$, $s_1 = 1.0$ mm, $\tau_f = 0.15\tau_u$, $N = 10^6$ cycles, $f = 0.01$ Hz). (a) Time-dependent crack width, (b) Distribution of stresses under maximum load, (c) Distribution of stresses under minimum load

estimation of the minimum crack width from the next simple formulation

$$w(t) = w_0 - \varepsilon_{cs}(t)s_r \quad (26)$$

where w_0 is the minimum crack width estimated assuming that $l_{b,unl} = s_r/2$. This result agrees with

the proposal of other authors (Bischoff 2001, Fields and Bischoff 2004) and the formulation of some codes of practice (Model Code).

5. Simplified equations and practical recommendations

The model of section 3 has shown that the cyclic bond deterioration leads to a situation of the reinforced concrete tie where the bond stress is constant ($-\tau_f$) between two adjacent cracks under minimum load. Eqs. (10) and (14) are therefore assumed to define the state of the tie under the permanent load, even though $\sigma_{smin} > \sigma_{min,lim}$ at the first cycle. If Eq. (14) provides the permanent crack width, the allowable permanent steel stress (σ_{per}) can be derived as a function of the required crack width (w_{per})

$$\sigma_{per} = \left[w_{per} - \frac{\tau_f s_r^2}{E_s \Phi} (1 + \rho n) \right] \frac{E_s}{s_r} \tag{27}$$

Furthermore, the crack width increase due to shrinkage may be introduced from Eq. (26). Hence

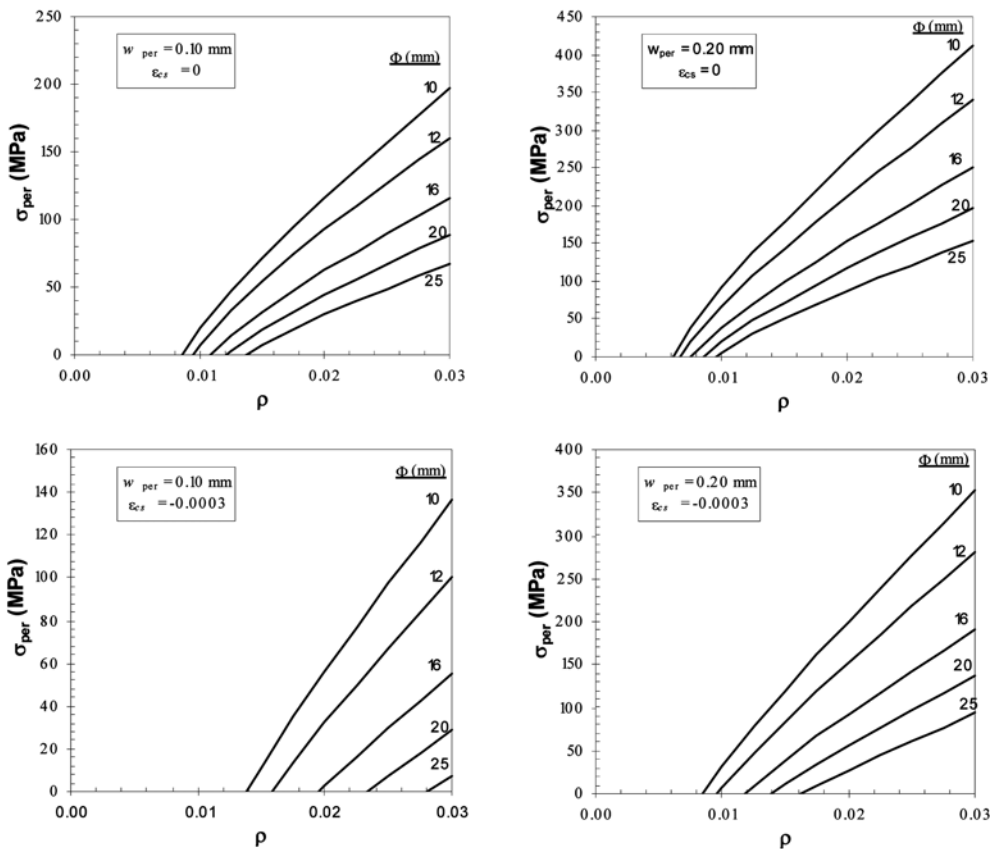


Fig. 16 Permanent stress as a function of ρ and Φ , with and without shrinkage ($f_c = 35$ MPa, $\tau_f = 0.15 \tau_u$, $\tau_u = 2f_c^{0.5}$).

$$\sigma_{per} = \left[w_{per} + \varepsilon_{cs} s_r - \frac{\tau_f s_r^2}{E_s \Phi} (1 + \rho n) \right] \frac{E_s}{s_r} \quad (28)$$

The limiting value of the crack width is specified by the codes of practice. It is however noted that some codes (Model Code) consider shrinkage strains in the crack width estimation and others do not (Eurocode). A consistent value of w_{per} should be therefore chosen. In the author's opinion, the limiting value of w_{per} should be fixed from environmental and aesthetic requirements regardless of the loads causing the cracks. All the cracking sources (mechanical, thermal, etc.) should be in turn included in the crack width estimation.

Eq. (28) can be used to obtain practical diagrams of the allowable permanent stress as a function of several parameters. Fig. 16 shows the role played by the steel reinforcement ratio and the bar diameter. The crack spacing is estimated according to the Model Code ($s_r = \Phi/(3.6\rho)$). The diagrams show that the allowable stress increases as the steel reinforcement ratio increases under a given value of the diameter. It is also observed that the allowable stress can be increased if a smaller diameter is used. The employ of closer, smaller bars is a generally accepted well-practice rule. Fig. 16 also indicates that the allowable stress decreases when the shrinkage is included.

Eq. (28) shows that the negative tension stiffening term is highly dependent on τ_f , which is a poorly investigated parameter. Values of 0.15-0.25 τ_u have been considered in the literature. τ_u is in turn dependent on f_c with a considerable scatter. A simplified value for τ_f as a function of f_c would be required for practical applications.

6. Conclusions

The paper has presented a model to study the effect of repeated loads on the reinforced concrete tie, focusing on the behaviour under minimum load and the explanation of the negative tension stiffening effect. From the present approach the following conclusions may be drawn:

1. Repeated loads reduce the contribution of concrete in tension between cracks under maximum load and lead to negative tension stiffening effect under minimum load. The crack width and the average strain are therefore larger than those given by the fully cracked member (bare steel).
2. Neglecting the tension stiffening effect under minimum load leads to unsafe design results since it has a negative contribution. The formulations of the codes of practice should be revised to properly include the negative tension stiffening influence for elements under repeated load. Many reinforced concrete members are actually subjected to this loading type, due to traffic, waves or wind.
3. Further research is needed in order to define the negative frictional strength (τ_f), provided this parameter has a considerable influence on the negative tension stiffening effect.
4. Simplified diagrams have been given in the paper in order to provide practical recommendations to estimate the permanent crack width and the allowable permanent stress in members subjected to repeated loading. The development of such diagrams is useful in the predimensioning stage to understand the reduction of the allowable permanent stress due to negative tension stiffening.

References

- Balazs, G.L. (1991), "Fatigue of bond", *ACI Mater. J.*, **88**(6), 620-629.

- Balazs, G.L. (1993), "Cracking analysis based on slip and bond stresses", *ACI Mater. J.*, **90**(4), 340-348.
- Beeby, A.W. and Scott, R.H. (2006), "Mechanisms of long-term decay of tension stiffening", *Mag. Concrete Res.*, **58**(5), 255-266.
- Bischoff, P.H. (2001), "Effects of shrinkage on tension stiffening and cracking in reinforced concrete", *Can. J. Civil Eng.*, **282**, 363-374.
- Blaschke, F. and Mehlhorn, G. (1995), "Verbundverhalten zwischen Stahl und Beton unter schwellender Belastung im Gebrauchslastbereich", *Beton- und Stahlbetonbau*, **90**(3), 77-79.
- CEB - FIP (1991), *CEB - FIP Model Code (1990)*, Lausanne, Switzerland.
- CEN (2004), *Eurocode EC-2. prEN 1992-1-1:2004*, Brussels, Belgium.
- Chan, H.C., Cheung, Y.K. and Huang, Y.P. (1992), "Crack analysis of reinforced concrete tension members", *J. Struct. Eng.*, ASCE, **118**(8), 2118-2132.
- Cornelissen, H.A.W. and Reinhardt, H.W. (1984), "Uniaxial tensile fatigue failure of concrete under constant amplitude and programme loading", *Mag. Concrete Res.*, **36**(129), 219-226.
- Fernández Ruiz, M. (2003), *Evaluación no lineal de los efectos estructurales producidos por las deformaciones diferidas del hormigón y el acero*, Ph.D. Thesis, Universidad Politécnica de Madrid.
- FIB (2000), *Bond of Reinforcement in Concrete. State of the Art Report. Bulletin no. 10*, federation internationale du beton, Lausanne, Switzerland.
- Fields, K. and Bischoff, P.H. (2004), "Tension stiffening and cracking of high-strength reinforced concrete tension members", *ACI Struct. J.*, **101**(4), 447-456.
- Ghali, A. and Favre, R. (1994), *Concrete Structures: Stresses and Deformations*, E & FN SPON Editions,
- Gilbert, I.R. (2007), "Tension stiffening in lightly reinforced concrete slabs", *J. Struct. Eng.*, ASCE, **133**(6), 899-903.
- Günther, G. and Mehlhorn, G. (1990). "Tension-stiffening, crack spacings, crack widths and bond-slip", *Protection of Concrete*, London, UK, 589-600.
- Gómez Navarro, M. and Lebet, J.P. (2001), "Concrete cracking in composite bridges: tests, models and design proposals", *Struct. Eng. Int.*, **11**(3), 184-190.
- Kaklauskas, G. and Ghaboussi, J. (2001), "Stress-strain relations for cracked tensile concrete from RC beam tests", *J. Struct. Eng.*, **127**(1), 64-73.
- Kreller, H. (1990), *Zum nichtlinearen Trag- und Verformungsverhalten von Stahlbetonstabtragwerken unter Last- und Zwangseinwirkung*, Deutscher Ausschuss für Stahlbeton. Heft 409, Universität Stuttgart, Germany.
- König, G. and Fehling, E. (1988), "Zur Rissbreitenbeschränkung im Stahlbetonbau", *Beton- und Stahlbetonbau*, **6** /1988 (161-167) - 7/1988 (199-204).
- Marti, P., Álvarez, M., Kaufmann, W. et al. (1998), "Tension chord model for structural concrete", *Struct. Eng. Int.*, **8**(4), 287-298.
- Morita, S. and Kaku, T. (1973), "Local bond-stress relationship under repeated loading", *IABSE Symposium, Resistance and Ultimate Deformability of Structures Acted on by Well Defined Repeated Loads*, Lisbon, Portugal, 221-226.
- Muttoni, A. and Fernández Ruiz, M. (2007), "Concrete cracking in tension members and application to deck slabs of bridges", *J. Bridge Eng.*, ASCE, **12**(5), 646-653.
- Oh, B.H. and Kim, S.H. (2007), "Realistic models for local bond stress-slip of reinforced concrete under repeated loading", *J. Struct. Eng.*, ASCE, **133**(2), 216-224.
- Plaines, P., Tassios, T. and Vintzeleou, E. (1982), "Bond relaxation and bond-slip creep under monotonic and cyclic actions", *Proceedings of the International Conference*, Paisley, France, 193-204.
- Pochanart, S. and Harmon, T. (1989), "Bond-slip model for generalized excitations including fatigue", *ACI Mater. J.*, **86**(5), 465-474.
- Rehm, G. and Eligehausen, R. (1979), "Bond of ribbed bars under high cycle repeated loads", *ACI J.*, **76**(15), 297-309.
- Sippel, T. (1996), *Zum Trag- und Verformungsverhalten von Stahlbetontragwerken unter Betriebsbelastung*, Ph.D. Thesis, Technische Universität Stuttgart, Germany.
- Tassios, T.P. and Yannopoulos, P.J. (1981), "Analytical studies on reinforced concrete members under cyclic loading based on bond stress slip relations", *ACI J.*, **78**(3), 206-216.
- Vecchio, F.J. (2000), "Disturbed stress field model for reinforced concrete: formulation", *J. Struct. Eng.*, ASCE,

126(9), 1070-1077.

Vecchio, F.V. and Collins, M.P. (1986), "The modified compression-field theory for reinforced concrete elements subjected to shear", *ACI J.*, **83**(2), 219-231.

Yankelevsky, D.Z., Jabareen, M. and Abutbul, A.D. (2008), "One-dimensional analysis of tension stiffening in reinforced concrete with discrete cracks", *Eng. Struct.*, **30**(1), 206-217.

Notations

A_c	: effective concrete area
A_s	: bar area
b	: parameter to define the cyclic rate of the relative slip increase
E_c	: modulus of elasticity of concrete
E_s	: modulus of elasticity of steel
F	: axial force
F_{cr}	: cracking load
F_{max}, F_{min}	: maximum and minimum force, respectively
$F_{min,lim}$: limit minimum force
f	: load frequency
f_c	: concrete compressive strength
f_{ct}	: concrete tensile strength
$l_{b,unl}$: unloaded transfer length
N	: number of cycles
n	: ratio between modulus of elasticity of steel and concrete
s	: relative slip
s_0	: static relative slip
s_{N_j}	: relative slip after N_j load cycles
s_r	: crack spacing
s_1	: relative slip that corresponds to the bond strength
s_2, s_3	: relative slips that correspond to changes in the form of the bond-slip law
t	: time
U_s	: bar perimeter
w	: crack width
w_0	: static crack width
w_{max}, w_{min}	: maximum and minimum crack width
w_{per}	: permanent crack width
w_{res}	: residual crack width
x	: abscissa
α	: shape factor of the bond-slip law
ΔF	: restraining force
ΔF_b	: fraction of the load transferred by bond stresses
ΔN_j	: number of cycles of step j
Δs_i^j	: slip increase of step j at node i
Δt_j	: time interval of step j
$\Delta \sigma_1$: steel stresses transferred from the steel to the concrete under maximum load
$\Delta \sigma_2$: steel stresses transferred from the steel to the concrete under minimum load
$\Delta \sigma_c$: compressive stresses transferred from the steel to the concrete
$\Delta \tau_i^j$: bond stress of step j at node i
$\Delta \sigma_c$: maximum difference of concrete strain along the crack spacing
$\Delta \varepsilon_{cs}$: increment of shrinkage strain
$\Delta \varepsilon_s$: maximum difference of steel strain along the crack spacing
ε_c	: concrete strain

ε_{cm}	: average concrete strain
ε_{cs}	: shrinkage strain
ε_{res}	: residual average steel strain
ε_s	: steel strain
ε_{sm}	: average steel strain
$\varepsilon_{smax}, \varepsilon_{smin}$: maximum and minimum steel strain at the crack, respectively
Φ	: bar diameter
ρ	: steel reinforcement ratio
σ_c	: concrete stress
$\sigma_{min,lim}$: limit minimum stress
σ_s	: steel stress
$\sigma_{smax}, \sigma_{smin}$: maximum and minimum steel stress at the crack, respectively
σ_{per}	: permanent steel stress at the crack
τ	: bond stress
τ_f	: negative frictional bond strength
τ_{max}, τ_{min}	: maximum and minimum bond stress, respectively
τ_{Nj}	: bond stress after N_j load cycles
τ_u	: ultimate bond strength
τ_{res}	: residual bond strength

Appendix

Eq. (5) can be rewritten in the form

$$\frac{d^2s}{dx^2} = Ks^\alpha \quad (\text{A.1})$$

A new variable z can be introduced, such as $z = ds/dx$. Hence

$$z \frac{dz}{ds} = Ks^\alpha \quad (\text{A.2})$$

This equation can be easily integrated due to the fact that variables are separated

$$z = \left(\frac{2K}{1+\alpha} s^{1+\alpha} + A \right)^{1/2} \quad (\text{A.3})$$

where A is a constant to be determined later. Variable z is now removed

$$\frac{ds}{dx} = \left(\frac{2K}{1+\alpha} s^{1+\alpha} + A \right)^{1/2} \quad (\text{A.4})$$

The integration of this equation is of the type

$$I = \int \frac{dx}{\sqrt{1+x^k}} \quad (\text{A.5})$$

This binary equation has an explicit solution only when $(1/k-1)$ or $(-1/2 + 1/k-1)$ are integer numbers. A closed solution is possible when $A = 0$. To do it, the next boundary condition is required

$$\frac{ds}{dx}(x=0) = 0 \quad (\text{A.6})$$

which means $\sigma_s = \sigma_c$ in the section halfway between cracks. This condition is only valid in the crack formation stage. In this case, the relative slip can be obtained as follows

$$s(x) = \left[\frac{2(1-\alpha)^2(1+n\rho)\tau_u x^2}{(1+\alpha)E_s \Phi s_1^\alpha} \right]^{\frac{1}{1-\alpha}} \quad (\text{A.7})$$